
IGBTs IN RESONANT CONVERTERS

by R. Letor, S. Musumeci, F. Frisina

ABSTRACT

The aim of this paper is to give help to the designers of resonant converters in the selection of IGBTs for use in their circuits. A method of characterizing IGBTs in resonant converters is developed and used to obtain graphs demonstrating the dependence of the power losses of the IGBT on certain key parameters, the circuit topology and the application requirements.

1. INTRODUCTION

Resonant and quasi-resonant switching techniques have been widely used in high-frequency power conversion systems, leading to reductions in size, weight and power losses. By forcing the switching transitions to take place when there is either zero current through or zero voltage across the power switch allows the switching losses to be minimized. However, the necessary current or voltage rating of the device used is much higher than that required in a device used in a conventional hard-switching system, and so the devices are more expensive.

MOSFETs are often chosen for the power switch in soft-switching applications, due to their high speed and easy drive. However, for medium and high power applications, their high conduction losses begin to cause problems, and IGBTs begin to become more attractive. Even in hard-switching applications, their higher current density, lower saturation voltages and high reliability mean that they are often used to replace MOSFETs.

Although in the past few years a large number of applications have been developed and a number of product families introduced, the behaviour of IGBTs in resonant circuits is still poorly understood, and designers are often reluctant to use them in this type of application.

This paper presents guidelines for the selection of IGBT devices for resonant applications, taking into consideration circuit parameters such as topology, power, switching frequency and input-output voltage ratio.

2. RESONANT TOPOLOGIES

The idealised switching waveforms of a Zero-Current (ZC) converter are shown in figure 1; a) shows "half wave" operation, while b) shows "full wave" (similar waveforms can be visualised for Zero-Voltage (ZV) systems by simply substituting the current waveform for the voltage and vice versa).

The parameters which characterise the ZC switching waveforms in both modes of operation are:

- at turn on, the current slope (di/dt) and the maximum voltage (V_{off})
- during conduction, the peak current ($I_{C(max)}$) and the conduction time (t_{on})
- at turn off, the voltage rise delay time (t_{delay}) and the current slope (di/dt).

For a ZC converter, the above parameters have current in place of voltage, and vice versa.

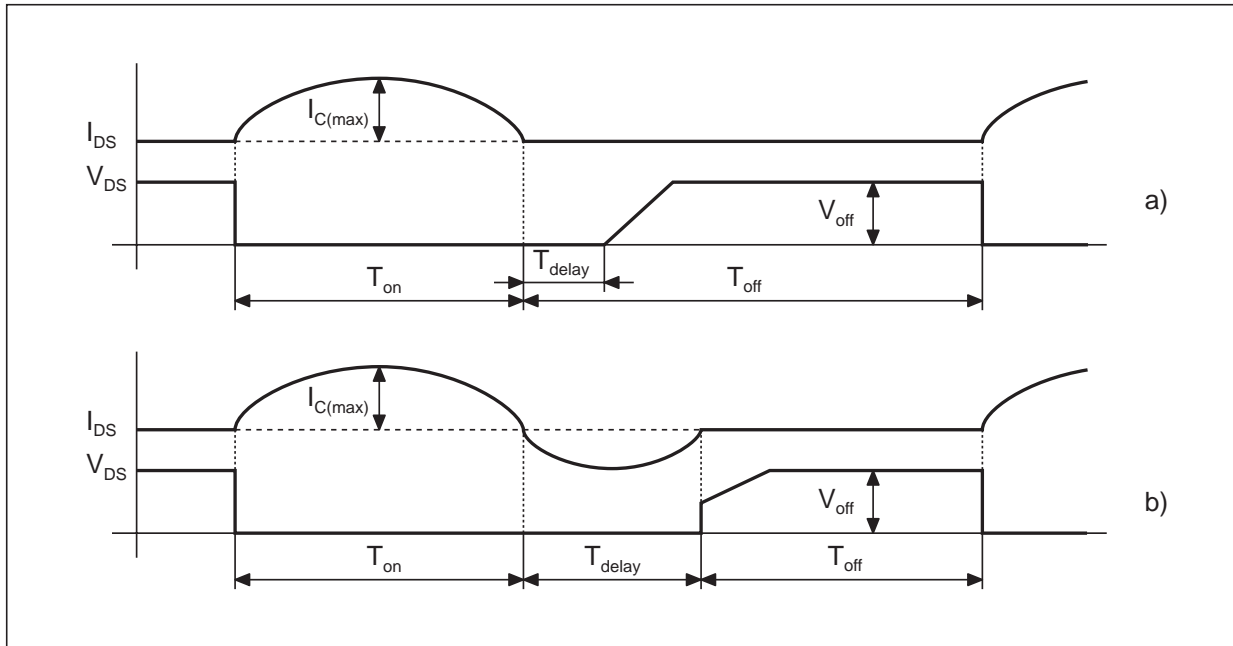
These parameters determine the power losses of the system, and second-order effects during the switching transients. The approach followed in this paper is to examine separately the effect of each of these key parameters on the behaviour of a number of different commercially available IGBTs in soft-switching applications.

3. IGBT DEVICES

The current density of an IGBT is higher than that of a Power MOSFET with the same voltage rating, particularly in the case of high voltage devices, as the on-voltage and hence conduction loss of the device is considerably lower. However, in hard-switching applications the switching losses of the IGBT can be much higher due to the effect of the "tail current" (see reference [6]), which results from the delay in turn-off of the bipolar section of the IGBT caused by the slow recombination of the minority carriers in its base. In soft-switching applications these losses can be reduced significantly, if the switching times required are longer than the minority carrier lifetime.

APPLICATION NOTE

Figure 1. Idealized switching waveforms of a ZC converter: a) "Half Wave" mode b) "Full Wave" mode



A number of IGBT devices are commercially available with a variety of saturation voltages and fall times. Figure 2 shows how, by increasing the gain of the intrinsic bipolar transistor, it is possible to reduce the saturation voltage, at the cost of increased fall time. The IGBTs considered in this paper are characterised in the following way:

- IGBTs with a very low saturation voltage ($V_{CE(sat)} = 1.5V$, fall time = $2\mu s$);
- Standard IGBTs ($V_{CE(sat)} = 2.2V$, fall time = $0.8\mu s$)
- Fast IGBTs ($V_{CE(sat)} = 3.2V$, fall time = $0.3\mu s$)

4. CHARACTERIZATION OF IGBTs

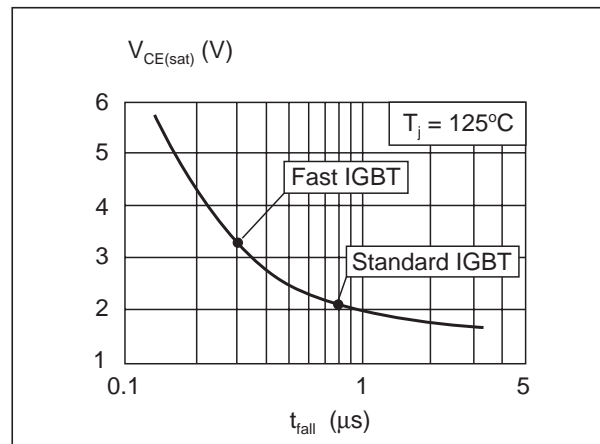
4.1 Test circuits

Figure 3 shows two circuits useful for the characterisation of IGBTs. a) shows a ZV test circuit, while b) shows a ZC circuit. The circuits allow simulation of a wide variety of operating conditions, and allow the di/dt and the maximum switching current to be controlled separately.

It should be noted that in ZV switchings the initial voltage can be negative, and the di/dt must be kept high.

In this case the Power MOSFET S1 is used to control the di/dt and the maximum current. In ZC switchings the di/dt is lower than is the case with ZV,

Figure 2. Standard vs. fast IGBTs



and depends upon both the resonant frequency and the maximum load current. The di/dt is controlled by means of the inductor L.

Figure 4 shows circuits to examine turn-off transients in a) ZV and b) ZC circuits. These circuits allow the di/dt , dv/dt and the voltage rise delay time to be controlled separately.

In the ZV resonant converter the parameters which influence the power losses most at turn-off are the collector current and the dv/dt - the di/dt is large enough to have no influence on the switching power losses.

Figure 3. Investigating turn-on: a) Test circuit for ZV turn-on b) Test circuit for ZC turn-on
c) ZV turn-on waveforms d) ZC turn-on waveforms

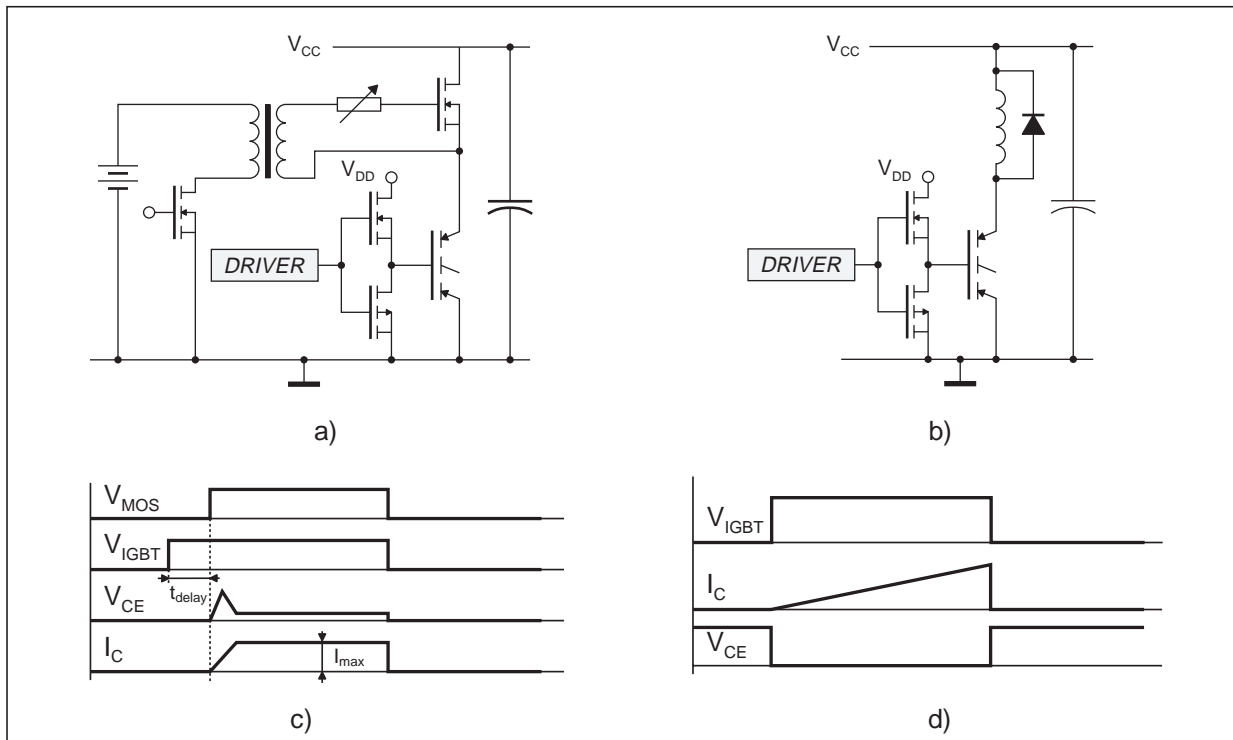
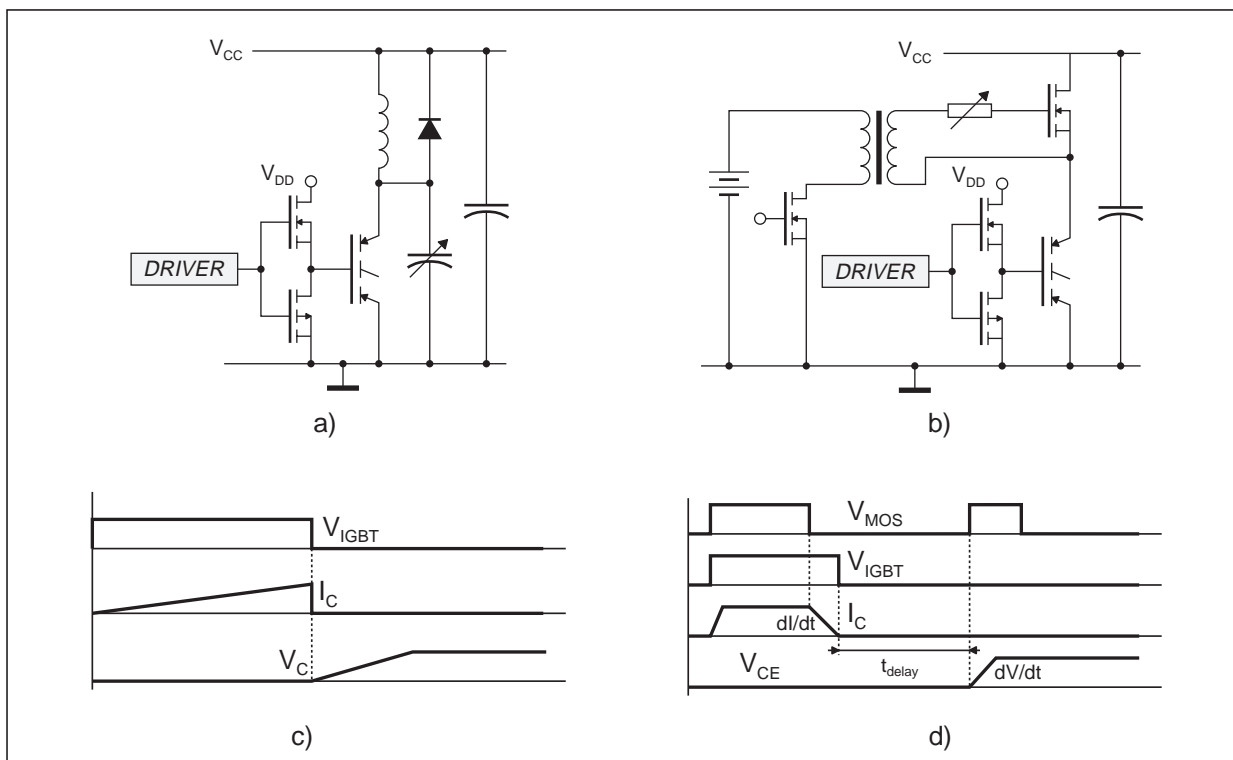


Figure 4. Investigating turn-off: a) Test circuit for ZV turn-off b) Test circuit for ZC turn-off
c) ZV turn-off waveforms d) ZC turn-off waveforms



APPLICATION NOTE

4.2 Experimental Results

Figure 5 shows collector current, dynamic saturation voltage and power loss waveforms for ZV turn-on. It can be seen that the peak value of the switching power losses is very similar to the value of the conduction losses. Figure 6 shows ZV turn-on losses for different values of current slope, with a fixed conduction current.

Figure 7 shows waveforms for the turn-on of the ZC circuit. The turn-on losses are very similar to those in the ZV circuit.

Figure 8 shows the influence of the current tail on the dv/dt at turn-off of the ZV circuit. Figure 9 shows the same waveform at various temperatures (note

the different order of magnitude on the power losses axis compared with figure 6). It can be seen that at very high junction temperatures the power losses begin to increase exponentially.

Figure 10 shows turn-off waveforms for ZC operation with various values of voltage rise delay time. Figure 11 shows that increasing the voltage rise delay time reduces the turn-off losses very quickly.

Figures 12 and 13 show the effects of di/dt and junction temperature on the power losses at turn-off for ZC operation.

Figures 14 and 15 compare the waveforms and turn-off losses of different IGBT types in ZC converters.

Figure 5. ZV turn-on waveforms at 125°C

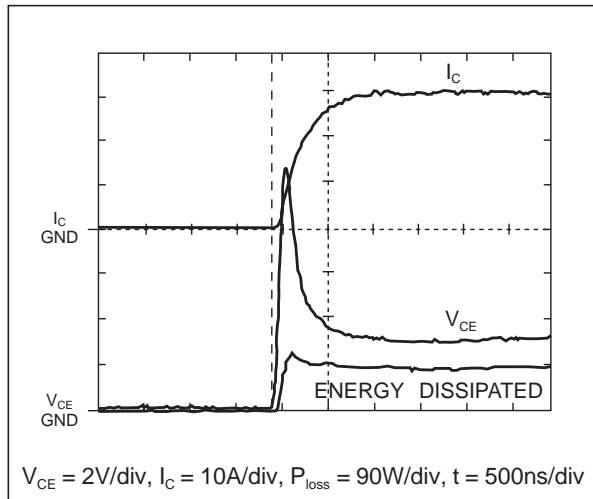


Figure 7. ZC turn-on waveforms at 25°C and 125°C

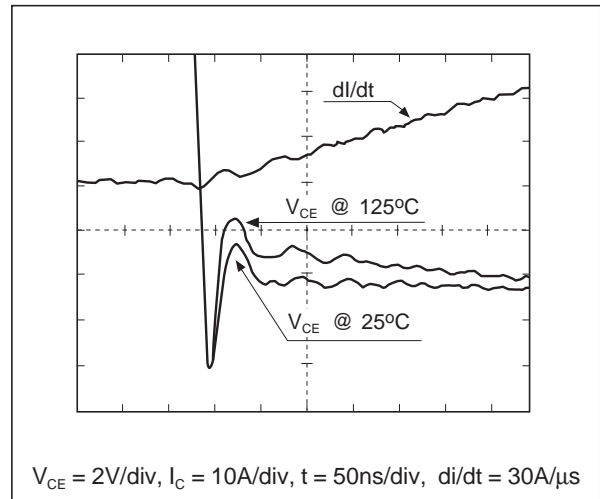


Figure 6. Variation of ZV turn-on losses with T_j , for various values of di/dt

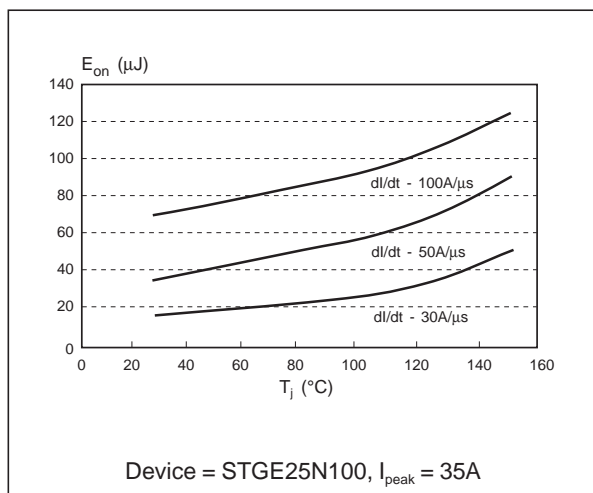


Figure 8. ZV turn-off waveforms at 150°C

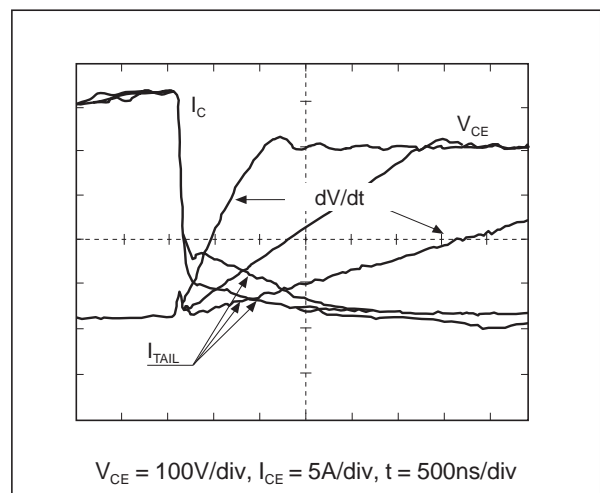


Figure 9. Variation of ZV turn-off losses with dV/dt , for various values of T_j

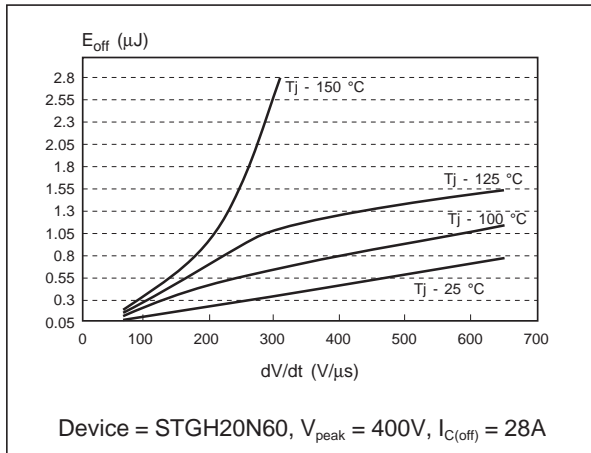


Figure 10. ZC turn-off waveforms at $100^\circ C$, varying the delay time. $di/dt = 18A/\mu s$

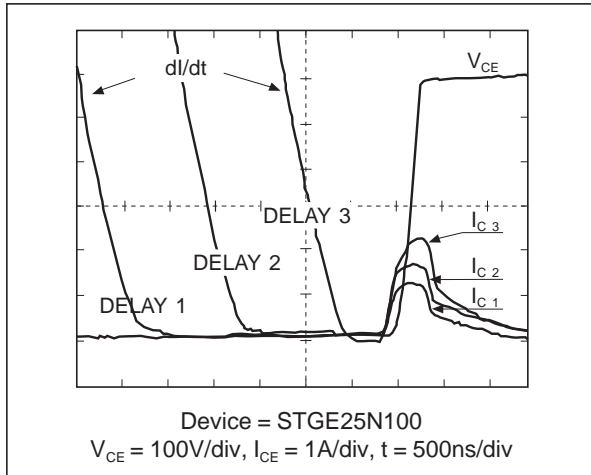


Figure 11. ZC turn-off losses against delay time, with various values of dI/dt

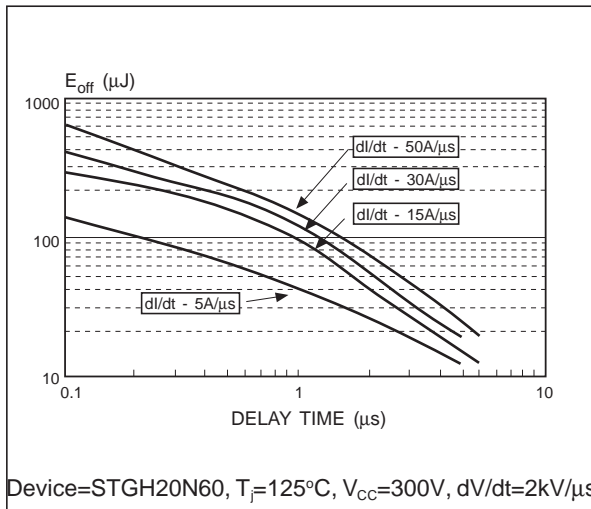


Figure 12. Variation of ZC turn-off losses with dI/dt , for various values of delay time

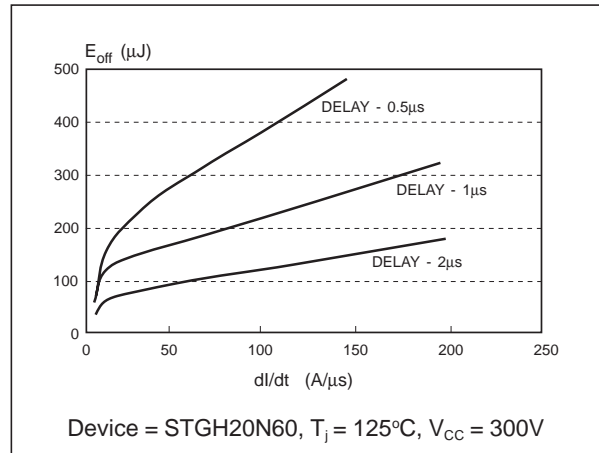


Figure 13. Variation of ZC turn-off losses with T_j , for various values of delay time

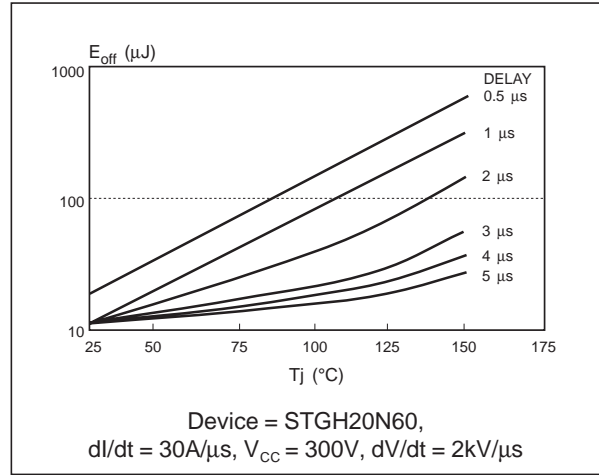


Figure 14. ZC turn-off waveforms for three types of IGBT

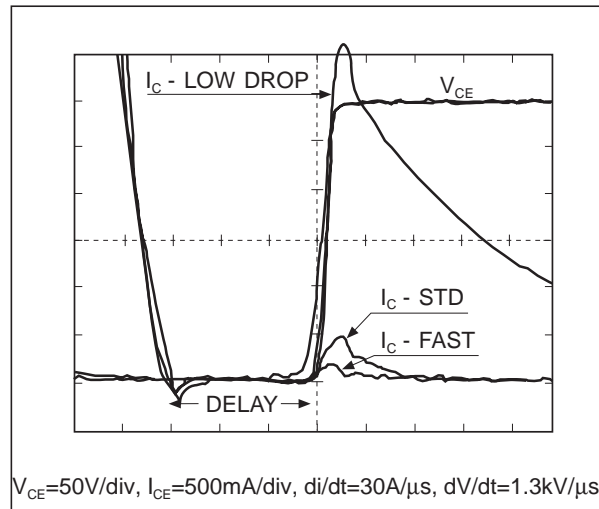
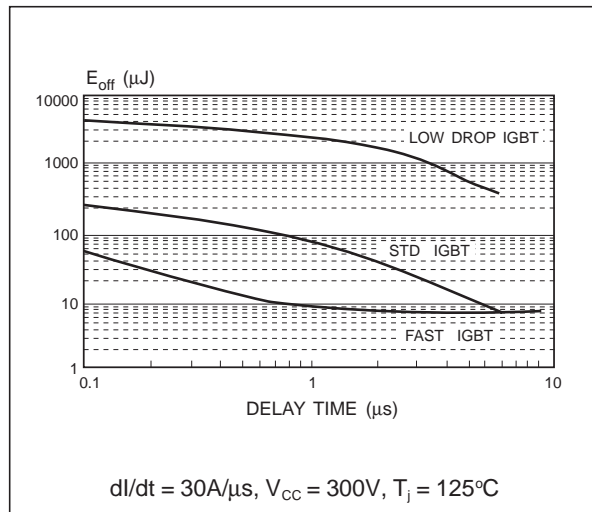


Figure 15. Comparison of turn-off losses of three types of IGBT with equal die size



5. USING THE RESULTS OF THE CHARACTERIZATION

5.1 Evaluation of turn-on losses

As shown above, the power losses are much lower at turn-on than at turn-off. It can also be seen from figure 5 that the energy loss waveform at turn-on is in the shape of a step; so as a first approximation the saturation voltage can be assumed to be a square wave with amplitude equal to its maximum value in the calculation of the turn-on losses.

5.2 Evaluation of turn-off losses

Calculation of the turn off losses requires evaluation of the following parameters:

- the di/dt
- the dv/dt
- the delay time.

These are determined by the design parameters of the converter such as the switching frequency f_s , the resonant frequency f_r , the voltage conversion ratio M , and the power ratings. As an example, for a buck ZC Quasi Resonant Converter (QRC) rated at 1.4kW with 300V input voltage and 100V output, these parameters may be:

$$M = f_s / f_r = 1/3 \rightarrow f_r = 3f_s$$

$$di/dt = 2\pi f I_{max} \text{ where } I_{max} = 2I_{out} = 28A$$

$$t_{on} = 1/2f_r$$

$$t_{delay} = t_{on} = t_r/2 = 1/2f_r$$

while for a buck ZV QRC rated at 1.4kW with 100V input and 70V output, they may be (assuming $V_{max} = 4 \times V_{min}$)

$$f_r = 1.5f_s / (1-M)$$

$$dv/dt = 2\pi f V_{max}$$

$$t_{on} / T = 1 - (f_s/f_r)$$

Different voltage ratings were chosen with the aim of comparing the behaviour of the same device in both resonant configurations, for converters having the same power ratings.

5.3 Power Losses vs Switching Frequency

Figure 16 shows the variation of power losses with frequency for a 600V - 20A IGBT in ZV operation, calculated using the values given in the examples of the previous section. It can be seen that the high voltage IGBT used (the ZV technique usually requires a high voltage device) has high switching losses even at low switching frequencies. Also, this application is characterized by a large duty cycle, increasing the conduction losses. As IGBTs seem to be more suited to ZC-QRCs, figure 17 compares the losses resulting from the use of a standard and a fast IGBT, along with a Power MOSFET with the same silicon size and voltage rating for comparison.

5.4 IGBTs and MOSFETs in ZC QRC

From figure 17 it follows that a MOSFET device requires a die size three or four times that needed by an IGBT in the same converter, in order to reduce the conduction losses to acceptable levels. However, on the other hand, IGBTs are affected much more by the switching frequency than MOSFETs. To calculate the optimum operating frequency of an IGBT, the maximum possible power dissipation in the application must first be calculated; the frequency can be found from figure 17.

As an example, with the set of conditions:

$$T_{amb} = 50^\circ C \quad T_{j(max)} = 125^\circ C$$

$$R_{th(heatsink)} = 3^\circ C/W \quad R_{th(j-c)} = 0.8^\circ C/W$$

the maximum possible power dissipation is:

$$P_{tot} = (T_{j(max)} - T_{amb}) / (R_{th(heatsink)} + R_{th(j-c)}) = 20W.$$

Figure 17 thus gives a maximum switching frequency of 100kHz for a standard IGBT, and 280kHz for a fast IGBT.

Figure 16. Variation of power losses with frequency for a ZV Buck QRC

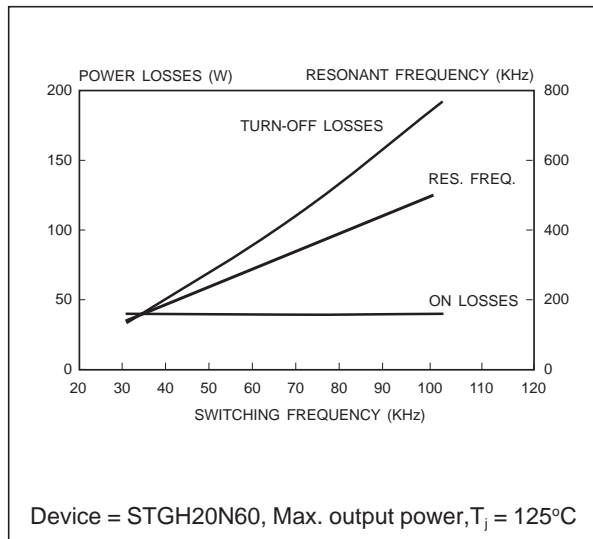
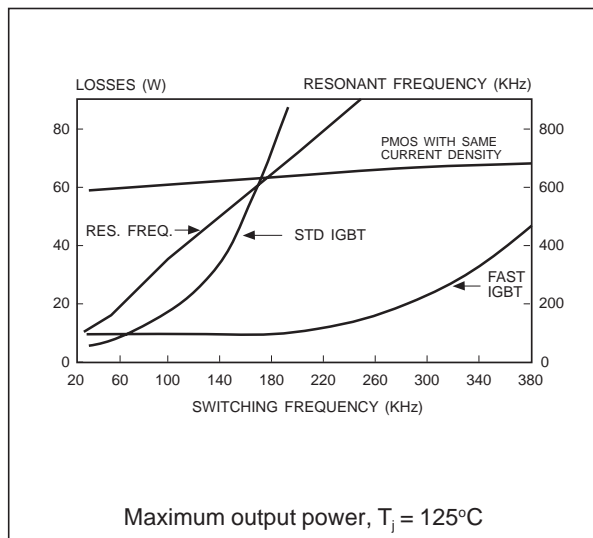


Figure 17. Comparison of losses for IGBT and MOSFET in a ZV Buck QRC



CONCLUSIONS

This paper presented a method of characterizing the behaviour of IGBTs in resonant converters. The switching characteristics of various types of IGBTs were examined, and the results used to obtain graphs of the variation of power losses with respect to various parameters. It was noted that:

- the switching losses are mainly affected by the bipolar transistor behaviour of the IGBT;
- as a first approximation, the losses related to the

dynamic saturation voltage can be included in the conduction losses for the frequency range considered;

- the "low drop" IGBT is not suited to use in this type of application due to its high switching losses;
- operating temperature is of key importance, due to the effects of the intrinsic bipolar of the IGBT.

Example applications were calculated using a buck QRC in both ZC and ZV operation. The ZC QRC proved to be the more attractive both for the lower voltage and current ratings required for the IGBT and the performance of the power switch under ZC conditions.

Possible switching frequency ranges were calculated for two types of IGBT, and also a Power MOSFET. It was shown that although the MOSFET can operate at much higher frequencies, it requires a much larger silicon area (and hence is more expensive) to keep down conduction losses to an acceptable level.

REFERENCES

- [1] "Resonant Switches - Topologies and Characteristics"
K. Liu, R. Oruganti, F. Lee
IEEE PESC, 1985, pp. 106-116
- [2] "Zero Voltage Switching Technique in DC/DC Converters"
K. Liu, F. Lee
IEEE PESC, 1986, pp. 58-70
- [3] "Synthesis and Analysis of DC/DC Power Converters"
D. Maksimovic
Ph.D. Thesis, Caltech, 1989
- [4] "Safe Behaviour of IGBTs subjected to dV/dt "
R. Lator, M. Melito
SGS-THOMSON Application Note AN476
- [5] "A 20kHz IGBT-Based Inverter With Improved Driver Circuits"
C. Cavallaro, A. Consoli, C. Licitra, S. Musumeci
UPEC '92 pp. 744-747
- [6] "An Introduction to IGBTs"
M. Melito, A. Galluzzo
SGS-THOMSON Application Note AN521

APPLICATION NOTE

Information furnished is believed to be accurate and reliable. However, STMicroelectronics assumes no responsibility for the consequences of use of such information nor for any infringement of patents or other rights of third parties which may result from its use. No license is granted by implication or otherwise under any patent or patent rights of STMicroelectronics. Specification mentioned in this publication are subject to change without notice. This publication supersedes and replaces all information previously supplied. STMicroelectronics products are not authorized for use as critical components in life support devices or systems without express written approval of STMicroelectronics.

The ST logo is a trademark of STMicroelectronics

© 1999 STMicroelectronics - Printed in Italy - All Rights Reserved

STMicroelectronics GROUP OF COMPANIES

Australia - Brazil - China - Finland - France - Germany - Hong Kong - India - Italy - Japan - Malaysia - Malta - Morocco -
Singapore - Spain - Sweden - Switzerland - United Kingdom - U.S.A.

<http://www.st.com>